Published in final edited form as:
Cell. 2009 December 11; 139(6): 1069–1083. doi:10.1016/j.cell.2009.11.030.

Nuclear Receptor-Induced Chromosomal Proximity and DNA Breaks Underlie Specific Translocations in Cancer

Chunru Lin[1,6], **Liuqing Yang**[1,6], **Bogdan Tanasa**[1], **Kasey Hutt**[2], **Bong-gun Ju**[1,5], **Kenny Ohgi**[1], **Jie Zhang**[1], **Dave Rose**[3], **Xiang-Dong Fu**[4], **Christopher K. Glass**[4], and **Michael G. Rosenfeld**[1,3,*]

[1] Howard Hughes Medical Institute University of California, San Diego School of Medicine, 9500 Gilman Drive, La Jolla, CA 92093-0648

[2] Bioinformatics Graduate Program, University of California, San Diego School of Medicine, 9500 Gilman Drive, La Jolla, CA 92093-0648

[3] Department of Medicine, Division of Endocrinology and Metabolism University of California, San Diego School of Medicine, 9500 Gilman Drive, La Jolla, CA 92093-0648

[4] Department of Cellular and Molecular Medicine University of California, San Diego School of Medicine, 9500 Gilman Drive, La Jolla, CA 92093-0648

[5] Department of Life Science, Sogang University, Seoul 121-742, Korea

Summary

Chromosomal translocations are a hallmark of leukemia/lymphoma and also appear in solid tumors, but the underlying mechanism remains elusive. By establishing a cellular model that mimics the relative frequency of authentic translocation events without proliferation selection, we report mechanisms of nuclear receptor-dependent tumor translocations. Intronic binding of liganded-AR first juxtaposes translocation loci by triggering intra- and interchromosomal interactions. AR then promotes site-specific DNA double-stranded breaks (DSBs) at translocation loci by recruiting two types of enzymatic machinery induced by genotoxic stress and liganded-AR, including Activation-Induced Cytidine Deaminase (AID) and the LINE-1 repeat-encoded ORF2 endonuclease. These enzymatic machineries synergistically generate site-selective DSBs at juxtaposed translocation loci that are ligated by Non-Homologous Ending Joining (NHEJ) pathway for specific translocations. Our data suggest that the confluence of two parallel pathways initiated by liganded-nuclear receptor and genotoxic stress underlie non-random tumor translocations, which may function in many types of tumors and pathological processes.

Keywords

Tumor Translocations; Prostate Cancer; Androgen Receptor; AID; PIWIL1; Nuclear Architecture; LINE-1 Repeats; ORF2; DNA Damage/Repair; LNCaP Cells

*To whom correspondence should be addressed:mrosenfeld@ucsd.edu.
[6]Denotes equal contribution

Introduction

Chromosomal translocations, caused by rearrangement of non-homologous chromosomes (Aplan, 2006), have been well described in leukemia and lymphomas (Greaves and Wiemels, 2003), but their occurrence in solid tumors is increasingly recognized, particularly in prostate cancer (Tomlins et al., 2005). It has been recognized that prevalent tumor translocations may be responsible for certain aggressive behaviors of prostate cancer (Wang et al., 2006). Androgen and its derivatives, which act *via* the androgen receptor (AR), are not only essential for development of the prostate gland, but also instrumental to prostate carcinogenesis (Heinlein and Chang, 2004). Recently, some high frequency gene fusion events have been discovered in prostate cancers, which involve translocation of the 5′ untranslated region of the AR target gene *TMPRSS2* to two members of the *ETS* family of genes *ERG* and *ETV1* (Tomlins et al., 2005). These gene fusion events, which may be present in 50-70% of prostate cancers, render specific members of the *ETS* family of genes under the control of androgens; such acquired androgen-dependent expression or overexpression of the *ETS* genes has been proposed to provide a key driving force to the development or aggressiveness of prostate cancers (Shaffer and Pandolfi, 2006).

While the linkage between chromosomal translocations and various forms of cancer has founded the theoretical grounds for cancer diagnosis and therapeutics, particularly for leukemia and lymphomas (Corral et al., 1996; Krivtsov and Armstrong, 2007), the underlying molecular mechanisms have remained incompletely understood. Although it is well established that transcriptionally active regions, such as promoters, can be particularly susceptible to DNA damage (Aguilera and Gomez-Gonzalez, 2008; Thomas and Rothstein, 1989), a prevalent view has been that tumor translocations may initially result from random chromosome rearrangement events, which are ultimately selected based on the proliferative and/or anti-apoptotic advantage provided by specific fusion gene products. However, precedents such as Gross Chromosomal Rearrangements (GCR) in yeast (Myung et al., 2001), V(D)J recombination, and Class Switch Recombination (CSR) during T and B cell development (Chaudhuri and Alt, 2004) argue for a role of genetically-based and cell lineage-specific juxtaposition of translocation loci, which may facilitate specific chromosomal translocations (Jhunjhunwala et al., 2008; Neves et al., 1999; Nikiforova et al., 2000; Roix et al., 2003). Because many types of cancer occur in tissues in which specific transcription factors may exert critical roles in tumor development, a potential mechanistic relationship between regulated transcription and the strategies that underlie tumor translocations, if any, remain an intriguing question.

Here, we present evidence that tumor translocations involving *TMPRSS2*, *ERG* and *ETV1* in prostate cancer are non-random events, which require two critical roles of AR: *(i)* ligand-dependent binding of AR to intronic binding sites near the tumor translocation sites, causing chromosomal movements that result in specific intra- and interchromosomal interactions to create the spatial proximity for tumor translocation partners, and *(ii)* the actions of intron-bound AR to both alter local chromatin architecture and recruit the ligand and genotoxic stress-induced enzymes, including the Activation-Induced cytidine Deaminase (AID) and LINE-1 repeat-encoded ORF2 endonuclease to these specific regions for facilitating DNA double-stranded breaks (DSBs) generation. The generated DSBs are subsequently ligated by the Non-Homologous End Joining (NHEJ) machinery. These findings elucidate several unexpected general principles for non-random chromosomal translocations in tumors.

Results

Androgens and Genotoxic Stress Synergistically Induce Prostate Cancer-Specific Chromosomal Translocations

Based on the critical roles of AR in prostate development and tumor progression, and the observation that genotoxic stress is able to rapidly induce chromosomal translocations (Deininger et al., 1998), we first investigated whether androgen treatment and genotoxic stress, either alone or in combination, might induce chromosomal translocations of *TMPRSS2:ERG* and *TMPRSS2:ETV1*. To establish a cellular model, we utilized androgen-responsive LNCaP prostate cancer cells in which these chromosomal translocations had not occurred (Tomlins et al., 2005).

Surprisingly, the treatment of LNCaP cells with both DHT (10^{-7} M) and irradiation (IR) (50 Gy) dramatically induced both *TMPRSS2:ERGb* and *TMPRSS2:ETV1b* fusion transcripts in 24hr, with similar effects reproducibly observed at lowered levels of DHT (10^{-9} M) and IR (10 Gy). (**Figures 1A** and **1B** and data not shown). Sequencing of induced fusion transcripts confirmed that they represented the authentic translocation fusion junctions (**Figures 1A** and **1B**). The cell viability did not differ significantly after 24hr treatment. *Actin* expression was equivalent among samples (Figure S1). Other modalities that cause genotoxic stress, including Etoposide and Doxorubicin, when combined with the DHT treatment, also induced tumor translocation (**Figures S3A** and **S3B**).

To quantitate the frequency at which each type of fusion transcript was formed, 48 individual sets of cells were exposed (24hr) to either DHT alone, IR alone, or both. RT-PCR analyses of *TMPRSS2:ERGb* and *TMPRSS2:ETV1b* fusion transcripts revealed that either treatment gave rise to a reproducible, but minimal, induction of the fusion transcripts, but the combined treatment exhibited an unequivocal, striking synergy (**Figures 1C** and **1D**). The frequency of these chromosomal translocations in LNCaP cells was estimated by dilution experiments to be ~1 event/10,000 cells (*vide infra*).

The finding that eight isoforms of *TMPRSS2:ERG* fusion transcripts have been identified in prostate cancer (Wang et al., 2006) led us to detect all potential induced fusion isoforms using primers targeting the first exon of *TMPRSS2* and the last exon of *ERG* or *ETV1*, respectively (**Figures 1E** and **1F**). This analysis revealed that the frequency of each induced *TMPRSS2:ERG* fusion isoform in LNCaP cells was very similar to that identified in prostate cancer tissues (Wang et al., 2006) (**Figures** 1E and S2). Together these data demonstrated that our cellular model and treatment conditions authentically recapitulate the *in vivo* chromosomal translocation events, and surprisingly, these specific patterns are established without proliferation selection.

To determine whether the generation of chromosomal translocation has cell type specificity, we analyzed IR-induced *BCR:ABL1* translocation in KG-1 cells (Deininger et al., 1998) (Figure S4A) and LNCaP cells. Although *BCR* and *ABL1* are expressed in LNCaP cells at a detectable level (**Figures S4B** and **S4C**), IR (50 Gy) induced *BCR:ABL1* fusion in KG-1 cells at an efficiency ~8-fold higher than that in LNCaP cells (Figure S4D). Conversely, irradiation of LNCaP cells induced *TMPRSS2:ERGb* or *TMPRSS2:ETV1b* fusion >10 fold more efficiently than in KG-1 cells under the same conditions (**Figures S4E** and **S4F**). These observations demonstrated that general genotoxic stress signals preferentially induce gene fusions in a non-random, cell type-specific fashion.

Using validated siRNAs to target specific components of the Homologous Recombination (HR), NHEJ, or Microhomology-Mediated End Joining (MMEJ) pathways (Figure S8A**)**, we found that knockdown of individual components of the NHEJ pathway generally attenuated

the induction of both *TMPRSS2:ERGb* and *TMPRSS2:ETV1b* fusion transcripts, suggesting the error-prone NHEJ as the major repair mechanism to generate fusion genes (Figure 1G). Removal of the major components of the HR pathway actually enhanced the induction of *TMPRSS2:ERGb* translocations (Figure 1H). Knockdown of individual components of several other DNA damage repair pathways did not show any significant effect on the chromosomal translocation types we tested (Figure S5 and data not shown).

Liganded-AR Induces Intra- and Interchromosomal Interactions Required for Translocations

Based on the dynamic re-organization of chromosomes during development or in response to specific signals (Cremer et al., 2006), we investigated whether one role of AR might be to mediate androgen-dependent spatial proximity of the corresponding chromosomal translocating regions. *ERG* and *TMPRSS2* are both located on Chromosome 21 (Chr21), ~3 megabases apart, while the *ETV1* gene is located on Chromosome 7 (Chr7). As *TMPRSS2* is a well-established direct AR target gene (Lucas et al., 2008), we tested whether DHT induced specific intra- and interchromosomal interactions between these regions.

To avoid potential complications associated with aneuploidy of cancer cells, we focused on normal prostate epithelial cells (PrEC). While *TMPRSS2* and *ERG* genes were independently localized in the nuclei of mock-treated PrEC cells, DHT stimulation (1hr) induced the apparent colocalization of these two genes in ~25% of cells, about half exhibiting mono-allelic interactions and the other half bi-allelic interactions as revealed by FISH analysis (Figure 2A). We performed a similar analysis for the *TMPRSS2* and *ETV1* genes in PrEC cells, which exhibited DHT-induced colocalization in ~10-15% of cells, the majority being mono-allelic interactions (Figure 2B). We observed similar induced colocalization in LNCaP cells (**Figure S6A** and **S6B**). In contrast, the *BCR* and *ABL1* gene loci did not show any DHT-dependent colocalization, suggesting the specificity of DHT-dependent chromosomal interactions (Figure S6C).

Based on the reported role of nuclear actin in transcriptional activation (Hofmann and de Lanerolle, 2006), we examined whether a nuclear myosin I (NMI)/actin-dependent mechanism might be involved in mediating intra- and interchromosomal interactions in PrEC cells, as recently documented for breast epithelial cells (Hu et al., 2008). Treatment of DHT-stimulated PrEC cells with Jasplakinolide (Jpk), which specifically inhibits depolymerization of actin networks (Holzinger, 2001), caused almost a complete loss of DHT-induced interchromosomal (*TMPRSS2:ETV1)* interactions, but did not affect intrachromosomal (*TMPRSS2:ERG*) interactions (**Figures 2C** and **2D**). Likewise, single-cell nuclear microinjection of siRNA that specifically targeted *NMI* (Grummt, 2006) had little effect on intrachromosomal (*TMPRSS2:ERG*) interactions, but caused a complete loss of the DHT-induced *TMPRSS2:ETV1* interchromosomal interactions (**Figures 2E** and **2F**). Similar results were also obtained by single-cell nuclear microinjection of a neutralizing antibody against NMI, which could be functionally rescued by co-injecting a plasmid expressing wild-type NMI, but not mutant NMI that fails to bind to ATP (Wang et al., 2003)(**Figures** 2G and S7). LNCaP cells treated with Latrunculin (LtA), which blocks actin polymerization (Rizk and Walczak, 2005), or Jpk exhibited inhibition of induced *TMPRSS2:ETV1* translocations, as was observed using an siRNA that specifically targeted *NMI* **(Figures 2H** and **2I**). Together, these observations reveal the mechanistic link between ligand-induced, nuclear myosin/actin motor system-dependent interchromosomal proximity and tumor translocations.

Mapping *TMPRSS2:ERG* and *TMPRSS2:ETV1* Translocation Breakpoints

To identify the potential DSBs in the corresponding introns of the two translocation partners, we adapted a protocol of BrdU labeling by terminal deoxynucleotide transferase (TdT) (Ju et al., 2006) coupled with ChIP-seq analysis to detect potential DNA breaks in response to DHT,

genotoxic stress, or both. To test the potential efficacy of this protocol for high-throughput screening experiments, we took advantage of the inducible 4-OHT-I-PpoI systems to generate specific cleavage sites on Chromosome 1 (Berkovich et al., 2008) and labeled these sites with BrdU. Indeed, anti-BrdU ChIP assay showed that after induction with 4-OHT, both the 5′ and 3′ chromatin fragments at the cleavage site, but not the flanking region, could be labeled by BrdU (Figure S9). By applying this protocol to LNCaP cells, our data revealed one potential breakpoint located within or nearby intron 1 of the *TMPRSS2* gene (Region I), two potential breakpoints located within intron 3 of *ERG* gene (Regions II and III), and one potential breakpoint in the *ETV1* gene intron 3 (Region IV) (Figure 3A). Compared to mock treatment, DHT induced an ~ 6-10-fold change at each of these putative DSBs (Figure 3B). These putative sites were further confirmed by conventional ChIP analysis, in DHT or DHT+IR treated LNCaP cells (**Figures 3C** and **3D**).

As illustrated in Figure 3A, amplification with primer pairs flanking Region II and I resulted in a single PCR product (**Figure 3E**, band *a*) containing a breakpoint between nucleotides Chr21: 38819940-38819946 on *ERG* gene and nucleotide Chr21: 41792689-41792695 on *TMPRSS2* gene (Figure 3E), which confirms that the DNA breaks identified in these pilot experiments corresponded to actual translocation breakpoints in these genes. Taking advantage of a finding that simultaneous cotransfection of FLAG-DOT1L (encoding an H3K79 methyltransferase) expression plasmid and *MeCP2* siRNA into LNCaP cells resulted in a 60-fold induction of fusion transcript (Figure S10), we amplified two additional PCR products (**Figure 3F**, band *b* and *c*) using primer pair flanking Region III and I, finding that band *b* contains breakpoints between Chr21: 38840448-38840454 and Chr21: 41792689-41792695, and band *c* contains breakpoints between Chr21: 38840754-38840760 and Chr21: 41792689-41792695 (Figure 3F). Interestingly, both *ERG* and *TMPRSS2* utilize a common motif (TGT/AGGGA/T) for break/ligation (Figure 3H).

For *TMPRSS2:ETV1* translocation, two breakpoints between Chr7: 13991147-13991153 or Chr7: 13991182-13991188 and Chr21: 41798889-41798895 were revealed by sequencing PCR product *d* (**Figure 3G,** middle panel), containing a common CCAGG/CAA motif as their break/ligation sites (Figure 3I). An additional breakpoint between *ETV1* and *TMPRSS2* at Chr7: 13991254 and Chr21: 41791805 were identified from PCR product *e* (**Figure 3G,** lower panel). Together, these mapping results identified unique heptad repeats serving as breakpoints for non-random ligation sites of tumor translocation.

Sensitization of Intronic AR Binding Sites to Genotoxic Stress

Since AR agonists induced both intra- and interchromosomal movements that involved the AR target gene *TMPRSS2*, we hypothesized that the *ERG* gene might also harbor some previously unsuspected AR binding sites, even though *ERG* expression is not induced by AR agonists (Tomlins et al., 2005). Because the identified “break” sites in *ERG* and *TMPRSS2* are adjacent to potential Androgen Response Elements (AREs) or ARE half sites (**Figure 4A,** upper panel), we conducted conventional ChIP analysis for AR recruitment across the intronic translocation regions within the *ERG* and *TMPRSS2* genes. As controls, we observed the binding of AR to *PSA* promoter and to the recently identified ARE located 13.5kb upstream of the *TMPRSS2* gene (ARE V) (Wang et al., 2007), but no significant binding to either an AR negative binding region in the *TMPRSS2* gene (ARE III) (Wang et al., 2007) or the *GAPDH* exon8 region (Figure 4A). Interestingly, upon DHT treatment, we found that AR was clearly recruited to the *ERG* “break” site Region A (corresponding to Region II in Figure 3A), C and D (corresponding to Region III in Figure 3A), *TMPRSS2* “break” site Region F (corresponding to Region I in Figure 3A) and *ETV1* “break” site Region H (corresponding to Region IV in Figure 3A) with temporal kinetics similar to these observed at known positive AR binding sites (*PSA* promoter and *TMPRSS2* ARE V) (**Figures** 4A and S15A). AR was also recruited to a potential ARE (Region

G) 2.5 kb upstream of the *TMPRSS2* "break" site (Figure 4A). In contrast, the *ERG* Region B and the *TMPRSS2* Region E, neither of which harbor any apparent ARE nor serve as break sites, showed no significant AR recruitment (Figure 4A).

To understand the synergistic effect of liganded-AR and genotoxic stress on chromosomal translocation, we first examined the DNA damage response marked by γH2AX in DHT-, IR- or DHT+IR-treated LNCaP cells. No significant enrichment of γH2AX were detected at all the regions we tested with DHT alone; and a moderate recruitment was observed upon IR treatment alone with characteristic spreading to regions adjacent to DSBs. Surprisingly, there was a striking enrichment of γH2AX to the translocation regions (*ERG* Region A, C, D, the *TMPRSS2* Region F and the *ETV1* Region H) after combined treatment with DHT+IR (**Figures S11** and **S15B**). Since Ku80 protein binds to DNA DSBs, nicks, gaps and hairpins in a sequence-independent manner and serves as a key component of the NHEJ repair machinery (Critchlow and Jackson, 1998), we next applied Ku80 as a mark to validate site-specific DSBs at translocation regions. Consistently, we observed that Ku80 bound to the *TMPRSS2* and *ERG* intronic AR binding sites exclusively under the condition of combined treatment with DHT and IR, but not to control regions within the *ERG* gene (**Figures 4B**-**4D**). These results demonstrated a site-specific sensitization of AR-bound intronic sites to genotoxic stress-induced DSBs.

Because binding of nuclear receptors during transcriptional activation is characteristically accompanied by covalent histone modifications that mark structural changes of chromatin (Metivier et al., 2006), we next tested whether intronic AR binding causes histone modifications that facilitate sensitization of these regions to genotoxic stress. Enhanced H3K79 methylation, a mark of altered chromatin structure (Huyen et al., 2004) has been observed to correlate with V(D)J recombination in B cells (Ng et al., 2003). Histone H4K16 acetylation is also considered as a mark for chromatin relaxation (Shogren-Knaak et al., 2006) and is involved in DNA repair. We observed that DHT+IR provoked robust accumulation of di-methyl H3K79 and H4K16 acetylation markers in the *ERG* regions A, C, D and the *TMPRSS2* site F (**Figures S12A** and **S12B**). *TMPRSS2* ARE III and *GAPDH* exon 8 regions, at which no breaks occurred, provided negative controls. These data provide evidence that the androgen receptor acts to cause regional histone modifications at the intronic translocation sites.

As a 3′-5′ DNA helicase in yeast is required for GCR by enhancing binding of the replication protein A (RPA) (Banerjee et al., 2008), we tested whether binding of AR might induce the recruitment of RPA, which is known to bind to and stabilize single-stranded non-template DNA (Bochkarev and Bochkareva, 2004) by performing RPA ChIP analysis. Upon DHT stimulation for 1hr, RPA was rapidly recruited to the AR binding sites, persisting even after 16hr of DHT stimulation (Figure 4E). Consistent with a key role for RPA in yeast GCR, treatment of LNCaP cells with *RPA2* siRNA inhibited both intra- and interchromosomal translocations induced by DHT+IR (Figure 4F).

Genotoxic Stress-Induced Enzymatic Machinery Contributes to Chromosomal Breaks at Intronic AR Binding Sites

Although irradiation may cause random DSBs in the genome, we next investigate the roles of irradiation in generating site-specific DSBs at translocation regions. Recently, Gadd45, which is a well-known irradiation-induced protein, was shown to play an important role in mediating AID actions by forming a functional complex with AID (Rai et al., 2008). Gadd45 is also known to function as a transcriptional co-activator for a number of nuclear receptors (Yi et al., 2000). Normally, AID is expressed at a very low level in LNCaP cells; however, we observed that AR agonists and genotoxic stress both induced AID expression by ~3-fold and >60-fold, respectively (**Figures 5A** and **5B**). Correspondingly, the AID protein was highly induced in IR-treated cells as early as 4hr (Figure 5C).

We therefore tested the potential roles of DHT-dependent recruitment of AID/Gadd45 to AR, observing that AR interacted with both AID and Gadd45 upon DHT+IR treatment (Figure 5D). This interaction was DHT-dependent, because IR alone did not induce such interactions (Figure S13). These data suggested that the DHT- and IR-induced AID might be recruited to the intronic translocation sites *via* direct binding of the Gadd45/AID complex to liganded-AR. Indeed, ChIP analysis of anti-Myc-tagged AID (Figure S14A) revealed that AID was recruited to the intronic AR-binding sites on *ERG*, *TMPRSS2* and *ETV1* translocation regions, as well as to known AR targets such as *PSA* promoter and *TMPRSS2* enhancer, but not to non-AR binding sites (**Figures** 5E and S15C). To further confirm a functional role for AID and Gadd45 in AR dependent tumor translocations, we treated LNCaP cells with either DHT or Bicalutamide (Casodex, CDX) and observed only minimal recruitment of AID or Gadd45 to intronic AR binding sites in CDX-treated cells (**Figures 5F** and **5G**).

Because AID mediates CSR and Somatic Hypermutation (SHM) by initiating deamination of bases of single-stranded non-template DNA during transcription (Chaudhuri et al., 2003), we investigated whether recruitment of AID is essential for the generation of DSBs by monitoring the enrichment of Ku80 at the translocation regions under the condition of *AID* knockdown by siRNA (Figure S8B). Knockdown of *AID* resulted in a dramatic decrease in the Ku80 enrichment as shown by ChIP analysis (Figure 5H), indicating an inhibition of DSBs generation in these translocation regions. To further validate this finding, we also used the BrdU/TdT assay to confirm that DSBs generated at these intronic sites are mediated by AID (Figure 5I). Consistent with these observations, siRNA knockdown of *AID* blocked the induction of both intra- and interchromosomal translocations (Figures 5J). The actual frequency of chromosomal translocation events was quantitated by PCR analysis in serial dilution experiments, finding that the rate of translocation induced by DHT+IR within 24hr fell from ~12×10^{-5} in control siRNA samples to ~3×10^{-5} in *AID* siRNA knockdown samples (Figure 5K).

One hallmark of AID enzymatic activity is the induction of SHM (Honjo et al., 2002). PCR amplification and sequencing of the break region (*ERG* region A) following DHT+IR treatment revealed evidence of the C to U and G to A mutations characteristic of SHM (Figure 6A). These mutations were inhibited by knockdown of *AID* prior to the treatment, suggesting that AID is actively involved in the observed DSB generation at translocations sites. In adjacent control regions (*ERG* region B), only basal mutation rate was observed (Figure 6A). To examine the possibility that AID may also play an obligatory role in mediating AR-induced chromosomal movements, *AID* knockdown was performed in PrEC and LNCaP cells, finding that AID did not exert any effects on DHT-dependent interchromosomal movement, as revealed by FISH analysis (Figure S16).

We also observed that the Uracil-DNA Glycosylase (UNG), which recognizes the U•G mismatch generated upon deamination of cytidine by AID and generate abasic sites in the *C1* regions during CSR (Rajewsky and von Boehmer, 2008) localized to both *ERG* and *TMPRSS2* intronic AR binding sites in DHT+IR-treated LNCaP cells (Figure 6B). The recruitment of UNG was dependent on AID, indicated by reduced UNG recruitment following the knockdown of *AID* (Figure 6C).

To determine whether AID also plays a role in *SLC45A3:ETV1* chromosomal translocation identified in prostate cancer (Tomlins et al., 2007), we assessed these translocation events in DHT+IR-treated LNCaP cells following *AID* knockdown by specific siRNAs. With combined treatment of DHT and IR, we detected significant induction of *SLC45A3:ETV1* translocation in LNCaP cells, but not in PrEC cells, even though the expression of *SLC45A3* was similarly induced by DHT between these two cell lines (Figures S20 A-C). However, knockdown of *AID* abolished the induced *SLC45A3:ETV1* translocation (Figure S20D). Similarly, in B cell leukemia KG-1 cell line, the *BCR:ABL1* translocation is induced by high-dose irradiation, and

knockdown of *AID* caused a decrease in irradiation-induced *BCR:ABL1* translocation (**Figures S8D, S17A** and **S17B**), consistent with the previous report that AID is required for *c-Myc:IgH* translocation (Robbiani et al., 2008). While these findings strongly implicate the actions of AID to facilitate the DNA breaks at the intronic AR binding sites, they also raised the question whether other key enzymatic machinery was combinatorially required for induced chromosomal breaks.

Contribution of PIWI-Regulated LINE-1 Repeat/ ORF2 Endonuclease to Tumor Translocations

Intriguingly, DHT+IR was much less effective in inducing chromosomal translocations in PrEC cells than in LNCaP cells (Figures 6D, 6E and Figure S20B), even though the expression of the *TMPRSS2* and *SLC45A3* genes were induced similarly by DHT in both cell types (**Figures S18** and **S20C**). This observation is consistent with the possibility that cancer cells express additional factors that predispose to genome instability (Peng and Karpen, 2008). We therefore surveyed the mRNA expression levels of a series of "epigenetic" modulators that have been implicated in genome instability (Goldberg et al., 2007). Whereas the expression of most of these modulators did not change, a few (e.g. MOF1) did exhibit ~2-3-fold higher expression level in PrEC cells compared to LNCaP cells (data not shown), and *MOF* knock-down noticeably enhanced the efficiency of both intra- and interchromosomal translocations (Figure S19).

Strikingly, the most dramatic discrepant target we tested between LNCaP and PrEC cells was *PIWIL1* (~9-10 fold) (Figure 6F). PIWIs have been reported to suppress retrotransposition, including LINE-1 element during spermatogenesis (Aravin et al., 2007), but more recent studies have also implicated its role in somatic organs (Malone et al., 2009). Treatment of PrEC cells with *PIWIL1* siRNA caused induction of LINE-1 *ORF2* expression (**Figures** 6G and S8C). This finding raised the possibility that PIWIs might serve as an unexpected but key component of machinery that silences the expression of the LINE-1 encoded *ORF2* in normal prostate epithelial cells. Indeed, knockdown of *PIWIL1* enhanced the enrichment of γH2AX at *ERG* and *TMPRSS2* intronic translocation regions in PrEC cells (Figure 6H**)**. Despite its already low levels in LNCaP cells, further knockdown of *PIWIL1* elevated the DHT+IR-induced intra- and interchromosomal translocations (Figure 6I), whereas overexpression of PIWIs in LNCaP cells largely inhibited the induced chromosomal translocations (Figure 6J). Serial dilution experiment confirmed that the actual translocation frequency rose to ~39×10^{-5} in LNCaP cell following *PIWIL1* knockdown (Figure 6K).

A series of observations including the close relationship between LINE-1 element and genome instability (Prak and Haoudi, 2006), the potent endonuclease activity of LINE-1-encoded ORF2 (Goodier et al., 2004), and the activation of LINE-1 retrotransposition by irradiation (Farkash et al., 2006), led us to address the possibility that expression of the LINE-1-encoded ORF2 endonuclease might itself exert a direct role in tumor translocation. Indeed, the relative level of LINE-1 *ORF2* transcripts exhibited a significant (~6-fold) increase in LNCaP cells compared to PrEC cells, and *ORF2* expression was robustly induced by genotoxic stress (**Figures 7A** and **7B**). These data suggested that ORF2 might function as an additional irradiation/genotoxic stress-induced enzymatic machinery to mediate the chromosomal breaks involved in tumor translocations.

Consistent with this possibility, exogenous overexpression of LINE-1 ORF2 (Figure S14B) was sufficient to cause DHT-dependent DNA breaks at the established translocation sites, as revealed by specific recruitment of Ku80 to *ERG* and *TMPRSS2* intronic translocation regions, but not at other AR binding regions, such as *TMPRSS2* ARE III (Figure 7C). However, expression of an endonuclease-inactive mutant of ORF2 (Goodier et al., 2004) diminished the enrichment of Ku80 (Figure 7C). Furthermore, overexpression of the LINE-1 ORF2 induced

a marked increase in both intra- and interchromosomal translocations whereas the endonuclease-inactive mutant partially blocked DHT+IR-induced translocations (Figure 7D). Interestingly, overexpression of the endonuclease-inactive mutant of ORF2 reduced the DSBs generation marked by Ku80 recruitment at *ERG* and *TMPRSS2* intronic translocation regions in DHT+IR treated LNCaP cells, but with minimal effects on the recruitment of AID to the same regions (**Figures 7E** and **7F**). These data suggest that the LINE-1 ORF2 contributes to DSBs generation, in combination with the parallel actions of AID.

Indeed, ChIP analysis revealed that LINE-1 ORF2 was selectively recruited in a DHT-dependent fashion to the translocation regions, as well as to the enhancer region of *TMPRSS2*, but not to the promoter of *PSA* (Figure 7G**)**. However, we could not detect any direct physical interaction between AR and LINE-1 ORF2, suggesting the possibility that the recruitment of LINE-1 ORF2 may result from other events, including the AR-induced alterations in local chromatin architecture, and the exposed A/T-rich ssDNA that might then attract LINE-1 ORF2 to these chromatin regions. Importantly, the recruitment of ORF2 to translocation regions was not affected by removal of AID (Figure 7H), supporting the model that irradiation-induced LINE-1 ORF2 and AID act as independent mechanisms that combinatorially contribute to DSBs generation and tumor translocation. Thus, we conclude that activation of LINE-1 *ORF2* expression in tumor cells appears to provide an additional endonuclease activity that makes an important quantitative contribution to ligand/genotoxic stress-induced tumor translocations. The functional role of LINE-1 ORF2 in chromosomal translocation has been further extended based on our findings that overexpression of LINE-1 ORF2 endonuclease-inactive mutant abolished DHT+IR-induced *SLC45A3:ETV1* translocation (Figure S20E). Therefore, it is highly possible that LINE-1 ORF2 has a general function in facilitating chromosomal breaks and global genome instability in cancer cells.

Discussion

A long-standing concept in tumor translocations has been that genotoxic stress causes direct, random DSBs that lead to random translocations, with selection of those conferring growth advantage. Here, by devising and investigating a model of tumor translocations that fully mimics the frequency of *in vivo* events without proliferative selection, we suggested that, rather, there is a site-selective immediate pattern of DSBs that ultimately dictate the pattern of tumor translocations. This system has permitted the identification of several unexpected mechanisms, some sequential and others combinatorial, by which the androgen receptor acts in concert with genotoxic stress as parallel pathways to direct rapid, site-specific and cell type-specific tumor translocations in the absence of proliferative selection (Figure 7I). Translocation breakpoint preferences are dictated both by *(i)* site-specific binding of liganded-AR at intronic translocation regions that trigger rapid intra- and interchromosomal interactions, which results in spatial proximity required for translocations, and *(ii)* induced alterations of local chromatin architecture are permissive for sensitizing these regions to genotoxic stress. These transcription-related events, in combination with activation and induction of specific enzymatic machineries by ligand and genotoxic stress, mechanistically underlie the extended DNA breaks at the critical intronic AR binding sites. Thus, rather than being entirely the consequence of random damage-induced DSBs, with selection for the resulting tumor translocations that confer putative growth advantages as is commonly hypothesized, there appears to have an initial selective sensitization in a site-specific manner that presages the observed tumor translocations in prostate cancer. Therefore our findings suggest the provocative concept that liganded-receptor acts, in a sense, as a mutagen, licensed by the enzymatic machinery activated by genotoxic stress.

One initial puzzle was how the various *TMPRSS2* fusion partners were brought together for DNA recombination. We found that AR bound to multiple intronic regions near break sites in

TMPRSS2, *ERG* and *ETV1* genes, juxtaposing DNA breaks for subsequent recombination. This spatial proximity induced by a specific transcription program is reminiscent of the DNA rearrangement in developing B cells, thus suggesting that a general strategy is exploited for DNA rearrangement in tumorigenesis as well as during normal development. The requirements of a nuclear motor for the induced proximity permitted our demonstration that the induction of this spatial proximity is actually prerequisite for the induced translocation events.

Our data indicate that AR acts in concert with a number of key enzymes induced by androgens and genotoxic stress, including AID, previously considered to be a B cell-specific factor (Chaudhuri et al., 2003), Gadd45 and quite unexpectedly, the LINE-1-encoded ORF2, to license extended DSBs. AID is recruited to the intronic AR binding sites as part of the genotoxic stress-induced Gadd45/AID complex. These recruitments are postulated to be permissive for potentiating the occurrence of specific translocation breakpoints that we have mapped within the *TMPRSS2*, *ERG* and *ETV1* genes. Our data further suggest that only ~20% of intronic AR binding sites exhibiting induced DSBs. We have further documented that these breaks are marked by the recruitment of Ku80 and by direct incorporation of BrdU at these sites. The presence of micro-homology in multiple *TMPRSS2:ERG* and *TMPRSS2:ETV1* fusion sites lends further support for the model that there are staggered sites of DNA breakage as might be expected from the sequential actions of AID and UNG, analogous to their predicted functions in CSR (Stavnezer et al., 2008). Further, we observed the mutations characteristic of somatic hypermutation within the short region of AID binding sites, reflecting actions of AID at these intronic break sites. Consistent with our findings, AID has been recently reported to be required for *c-myc:IgH* translocations in B cells (Robbiani et al., 2008).

A key challenge was to identify specific machineries altered in tumors that might sensitize the cell to tumor translocations. The observation that the DHT+IR induced chromosomal translocations observed in prostate cancer cells were not detected in normal prostate epithelial cells led to the discovery of the critical, independent role of the PIWI-regulated LINE-1 encoded-ORF2 endonuclease in translocation events. Thus, in addition to the induction of AID in prostate cancer cells, we have uncovered a second, unexpected component of this sensitization mechanism based on the diminished expression of PIWIs, which serves as a dedicated protective strategy to block retrotransposition of LINE-1 elements to ensure genome stability in germ cells (O'Donnell and Boeke, 2007). Surprisingly, we found that the level of *PIWIL1* was dramatically lower (>9-fold) in LNCaP cells than in normal prostate epithelial cells. Even at this low level in LNCaP cells, knockdown with specific siRNA caused a further deprotection of the genome, resulting in increased chromosomal translocations.

To our surprise, even in the absence of genotoxic stress, the ORF2 endonuclease appears capable of targeting to the intronic AR bound sites to license DNA breakage, which emphasizes its independent, parallel function to AID in generating DSBs at the translocation sites. Our findings are consistent with the reported elevation of the LINE-1 ORF2 endonuclease activity in prostate cancer and the inducibility of this enzyme by irradiation (Farkash et al., 2006; Santourlidis et al., 1999), and also with the documented role of PIWIs in silencing LINE-1 repeat movement during neurogenesis (Muotri et al., 2005).

Because androgens exert important developmental roles in the prostate, we suggest that similar events might occur in other cancer types in which a selective, regulated DNA binding transcription factor(s) serves to promote DNA rearrangement. Finally, understanding the molecular mechanisms that underlie tumor translocations and specific “epigenetic” strategies used by normal cells to protect the genome against such deleterious DNA rearrangements have the promise to provide insights into the etiology of cancer and to facilitate the development of new diagnostic/therapeutic approaches.

Experimental Procedures

Cell Lines and Treatments

The prostate cancer cell line LNCaP was obtained from the American Type Culture Collection (ATCC). Human Prostate Epithelial Cells (PrEC) were obtained from Lonza and maintained in PrEGM media. Transfection of LNCaP cells with siRNA and plasmid DNA were performed using Lipofectamine2000™ (Invitrogen) and Nucleofector® Kit R (Lonza), respectively. Transfection of PrEC cells with siRNA was performed using DeliverX Plus siRNA transfection reagent (Panomics). MVA/T7RP-mediated expression of LINE-1 proteins was performed as previous described (Goodier et al., 2004). For induction of chromosomal translocation, LNCaP or PrEC cells were grown in charcoal-stripped serum containing media for 48 hr followed by mock, DHT (10^{-7} M), γ-irradiation (50 Gy) treatment, or both. After treatments, the cells were re-incubated for 24hr before being harvested for appropriate assays. Cell viability in cultures before and after irradiation was assessed by trypan blue exclusion.

Fluorescence *in situ* Hybridization

PrEC or LNCaP cells were stimulated with vehicle or 10^{-7} M of DHT for 1hr. Cell nuclei isolation and DNA-FISH was carried out according to a method previously described (Hu et al., 2008), and the probes were synthesized by Integrated DNA Technologies (IDT) and listed in Supplemental Table 1.

DNA-break Labeling and Chromatin Immunoprecipitation (ChIP)

The labeling of transient DNA break(s) by BrdU was performed as described (Ju et al., 2006). ChIP and Re-ChIP were performed as described previously (Shang et al., 2000). The enrichment of the DNA template was analyzed by QPCR using primers listed in Supplemental Table 1.

Single-Cell Nuclear Microinjection Assays

The single cell nuclear microinjection assays were performed as described (Perissi et al., 2004).

Data Analysis and Statistics

Relative quantities of *TMPRSS2:ERG* and *TMPRSS2:ETV1* fusion transcript were normalized to *Actin* and further to the expression level of *TMPRSS2*. The relative amount of each fusion transcript was then calibrated to DHT alone or DHT+IR treated control sample as appropriately. Calibrated quantities are indicated and samples without detectable fusion transcript after 40 cycles of amplification are indicated by 0 (Tomlins et al., 2007). Results are reported as mean ± SEM of three independent experiments. Comparisons were performed using two-tailed paired Student *t*-test. *$p<0.05$, **$p<0.01$, ***$p<0.001$.

Supplementary Material

Refer to Web version on PubMed Central for supplementary material.

Acknowledgments

We thank C. Nelson for various cell culture assistance; J. Hightower for artwork; D. Benson for assistance with the manuscript; Dr. V. Lunyak and Dr. X. Zhu for critical comments; Dr. M. Schwartz and E. Nunez for assistance with fluorescence microscopy and FISH technology; Dr. Y. Zhang for providing the FLAG-DOT1L construct, Dr. M. B. Kastan for providing HA-ER-I-PpoI construct, and Dr. J. L. Goodier for providing LINE-1 ORF1, ORF2 constructs, Ankara vaccinia virus that expresses T7 polymerase and polyclonal antibody against ORF2. Dr. S. Heinz for providing PIWIL1 and PIWIL2 expression constructs, and AstraZeneca for providing Casodex®. M.G.R. is a Howard Hughes Medical Institute Investigator. This study was funded by grants from NIH/NCI , DoD and Prostate Cancer Foundation

to M.G.R., X.D.F. and C.K.G. C. Lin is a Fellow of Susan G. Komen for the Cure (KG080247), and L. Yang is an awardee of Era of Hope Postdoctoral Award supported by DoD (GRANT00325108).

References

Aguilera A, Gomez-Gonzalez B. Genome instability: a mechanistic view of its causes and consequences. Nat Rev Genet 2008;9:204–217. [PubMed: 18227811]

Aplan PD. Causes of oncogenic chromosomal translocation. Trends Genet 2006;22:46–55. [PubMed: 16257470]

Aravin, AA.; Sachidanandam, R.; Girard, A.; Fejes-Toth, K.; Hannon, GJ. Science. Vol. 316. New York, NY: 2007. Developmentally regulated piRNA clusters implicate MILI in transposon control; p. 744-747.

Banerjee S, Smith S, Oum JH, Liaw HJ, Hwang JY, Sikdar N, Motegi A, Lee SE, Myung K. Mph1p promotes gross chromosomal rearrangement through partial inhibition of homologous recombination. The Journal of cell biology 2008;181:1083–1093. [PubMed: 18591428]

Berkovich E, Monnat RJ Jr. Kastan MB. Assessment of protein dynamics and DNA repair following generation of DNA double-strand breaks at defined genomic sites. Nature protocols 2008;3:915–922.

Bochkarev A, Bochkareva E. From RPA to BRCA2: lessons from single-stranded DNA binding by the OB-fold. Current opinion in structural biology 2004;14:36–42. [PubMed: 15102447]

Chaudhuri J, Alt FW. Class-switch recombination: interplay of transcription, DNA deamination and DNA repair. Nat Rev Immunol 2004;4:541–552. [PubMed: 15229473]

Chaudhuri J, Tian M, Khuong C, Chua K, Pinaud E, Alt FW. Transcription-targeted DNA deamination by the AID antibody diversification enzyme. Nature 2003;422:726–730. [PubMed: 12692563]

Corral J, Lavenir I, Impey H, Warren AJ, Forster A, Larson TA, Bell S, McKenzie AN, King G, Rabbitts TH. An Mll-AF9 fusion gene made by homologous recombination causes acute leukemia in chimeric mice: a method to create fusion oncogenes. Cell 1996;85:853–861. [PubMed: 8681380]

Cremer T, Cremer M, Dietzel S, Muller S, Solovei I, Fakan S. Chromosome territories--a functional nuclear landscape. Current opinion in cell biology 2006;18:307–316. [PubMed: 16687245]

Critchlow SE, Jackson SP. DNA end-joining: from yeast to man. Trends in biochemical sciences 1998;23:394–398. [PubMed: 9810228]

Deininger MW, Bose S, Gora-Tybor J, Yan XH, Goldman JM, Melo JV. Selective induction of leukemia-associated fusion genes by high-dose ionizing radiation. Cancer research 1998;58:421–425. [PubMed: 9458083]

Farkash EA, Kao GD, Horman SR, Prak ET. Gamma radiation increases endonuclease-dependent L1 retrotransposition in a cultured cell assay. Nucleic acids research 2006;34:1196–1204. [PubMed: 16507671]

Goldberg AD, Allis CD, Bernstein E. Epigenetics: a landscape takes shape. Cell 2007;128:635–638. [PubMed: 17320500]

Goodier JL, Ostertag EM, Engleka KA, Seleme MC, Kazazian HH Jr. A potential role for the nucleolus in L1 retrotransposition. Human molecular genetics 2004;13:1041–1048. [PubMed: 15028673]

Greaves MF, Wiemels J. Origins of chromosome translocations in childhood leukaemia. Nature reviews 2003;3:639–649.

Grummt I. Actin and myosin as transcription factors. Current opinion in genetics & development 2006;16:191–196. [PubMed: 16495046]

Heinlein CA, Chang C. Androgen receptor in prostate cancer. Endocrine reviews 2004;25:276–308. [PubMed: 15082523]

Hofmann WA, de Lanerolle P. Nuclear actin: to polymerize or not to polymerize. The Journal of cell biology 2006;172:495–496. [PubMed: 16476772]

Holzinger, A. Methods in molecular biology. Vol. 161. Clifton, NJ: 2001. Jasplakinolide. An actin-specific reagent that promotes actin polymerization; p. 109-120.

Honjo T, Kinoshita K, Muramatsu M. Molecular mechanism of class switch recombination: linkage with somatic hypermutation. Annual review of immunology 2002;20:165–196.

Hu Q, Kwon YS, Nunez E, Cardamone MD, Hutt KR, Ohgi KA, Garcia-Bassets I, Rose DW, Glass CK, Rosenfeld MG, et al. Enhancing nuclear receptor-induced transcription requires nuclear motor and

LSD1-dependent gene networking in interchromatin granules. Proceedings of the National Academy of Sciences of the United States of America 2008;105:19199–19204. [PubMed: 19052240]

Huyen Y, Zgheib O, Ditullio RA Jr. Gorgoulis VG, Zacharatos P, Petty TJ, Sheston EA, Mellert HS, Stavridi ES, Halazonetis TD. Methylated lysine 79 of histone H3 targets 53BP1 to DNA double-strand breaks. Nature 2004;432:406–411. [PubMed: 15525939]

Jhunjhunwala S, van Zelm MC, Peak MM, Cutchin S, Riblet R, van Dongen JJ, Grosveld FG, Knoch TA, Murre C. The 3D structure of the immunoglobulin heavy-chain locus: implications for long-range genomic interactions. Cell 2008;133:265–279. [PubMed: 18423198]

Ju, BG.; Lunyak, VV.; Perissi, V.; Garcia-Bassets, I.; Rose, DW.; Glass, CK.; Rosenfeld, MG. Science. Vol. 312. New York, NY: 2006. A topoisomerase IIbeta-mediated dsDNA break required for regulated transcription; p. 1798-1802.

Krivtsov AV, Armstrong SA. MLL translocations, histone modifications and leukaemia stem-cell development. Nature reviews 2007;7:823–833.

Lucas JM, True L, Hawley S, Matsumura M, Morrissey C, Vessella R, Nelson PS. The androgen-regulated type II serine protease TMPRSS2 is differentially expressed and mislocalized in prostate adenocarcinoma. The Journal of pathology 2008;215:118–125. [PubMed: 18338334]

Malone CD, Brennecke J, Dus M, Stark A, McCombie WR, Sachidanandam R, Hannon GJ. Specialized piRNA pathways act in germline and somatic tissues of the Drosophila ovary. Cell 2009;137:522–535. [PubMed: 19395010]

Metivier R, Reid G, Gannon F. Transcription in four dimensions: nuclear receptor-directed initiation of gene expression. EMBO reports 2006;7:161–167. [PubMed: 16452926]

Muotri AR, Chu VT, Marchetto MC, Deng W, Moran JV, Gage FH. Somatic mosaicism in neuronal precursor cells mediated by L1 retrotransposition. Nature 2005;435:903–910. [PubMed: 15959507]

Myung K, Chen C, Kolodner RD. Multiple pathways cooperate in the suppression of genome instability in Saccharomyces cerevisiae. Nature 2001;411:1073–1076. [PubMed: 11429610]

Neves H, Ramos C, da Silva MG, Parreira A, Parreira L. The nuclear topography of ABL, BCR, PML, and RARalpha genes: evidence for gene proximity in specific phases of the cell cycle and stages of hematopoietic differentiation. Blood 1999;93:1197–1207. [PubMed: 9949162]

Ng HH, Ciccone DN, Morshead KB, Oettinger MA, Struhl K. Lysine-79 of histone H3 is hypomethylated at silenced loci in yeast and mammalian cells: a potential mechanism for position-effect variegation. Proceedings of the National Academy of Sciences of the United States of America 2003;100:1820–1825. [PubMed: 12574507]

Nikiforova, MN.; Stringer, JR.; Blough, R.; Medvedovic, M.; Fagin, JA.; Nikiforov, YE. Science. Vol. 290. New York, NY: 2000. Proximity of chromosomal loci that participate in radiation-induced rearrangements in human cells; p. 138-141.

O'Donnell KA, Boeke JD. Mighty Piwis defend the germline against genome intruders. Cell 2007;129:37–44. [PubMed: 17418784]

Peng JC, Karpen GH. Epigenetic regulation of heterochromatic DNA stability. Current opinion in genetics & development 2008;18:204–211. [PubMed: 18372168]

Perissi V, Aggarwal A, Glass CK, Rose DW, Rosenfeld MG. A corepressor/coactivator exchange complex required for transcriptional activation by nuclear receptors and other regulated transcription factors. Cell 2004;116:511–526. [PubMed: 14980219]

Prak NL, Haoudi A. LINE-1 Retrotransposition: Impact on Genome Stability and Diversity and Human Disease. Journal of biomedicine & biotechnology 2006;2006:37049. [PubMed: 16877814]

Rai K, Huggins IJ, James SR, Karpf AR, Jones DA, Cairns BR. DNA demethylation in zebrafish involves the coupling of a deaminase, a glycosylase, and gadd45. Cell 2008;135:1201–1212. [PubMed: 19109892]

Rajewsky K, von Boehmer H. Lymphocyte development: overview. Current opinion in immunology 2008;20:127–130. [PubMed: 18513936]

Rizk RS, Walczak CE. Chromosome dynamics: actin's gone fishing. Curr Biol 2005;15:R841–842. [PubMed: 16243025]

Robbiani DF, Bothmer A, Callen E, Reina-San-Martin B, Dorsett Y, Difilippantonio S, Bolland DJ, Chen HT, Corcoran AE, Nussenzweig A, et al. AID is required for the chromosomal breaks in c-myc that lead to c-myc/IgH translocations. Cell 2008;135:1028–1038. [PubMed: 19070574]

Roix JJ, McQueen PG, Munson PJ, Parada LA, Misteli T. Spatial proximity of translocation-prone gene loci in human lymphomas. Nature genetics 2003;34:287–291. [PubMed: 12808455]

Santourlidis S, Florl A, Ackermann R, Wirtz HC, Schulz WA. High frequency of alterations in DNA methylation in adenocarcinoma of the prostate. The Prostate 1999;39:166–174. [PubMed: 10334105]

Shaffer DR, Pandolfi PP. Breaking the rules of cancer. Nature medicine 2006;12:14–15.

Shang Y, Hu X, DiRenzo J, Lazar MA, Brown M. Cofactor dynamics and sufficiency in estrogen receptor-regulated transcription. Cell 2000;103:843–852. [PubMed: 11136970]

Shogren-Knaak, M.; Ishii, H.; Sun, JM.; Pazin, MJ.; Davie, JR.; Peterson, CL. Science. Vol. 311. New York, NY: 2006. Histone H4-K16 acetylation controls chromatin structure and protein interactions; p. 844-847.

Stavnezer J, Guikema JE, Schrader CE. Mechanism and regulation of class switch recombination. Annual review of immunology 2008;26:261–292.

Thomas BJ, Rothstein R. Elevated recombination rates in transcriptionally active DNA. Cell 1989;56:619–630. [PubMed: 2645056]

Tomlins SA, Laxman B, Dhanasekaran SM, Helgeson BE, Cao X, Morris DS, Menon A, Jing X, Cao Q, Han B, et al. Distinct classes of chromosomal rearrangements create oncogenic ETS gene fusions in prostate cancer. Nature 2007;448:595–599. [PubMed: 17671502]

Tomlins, SA.; Rhodes, DR.; Perner, S.; Dhanasekaran, SM.; Mehra, R.; Sun, XW.; Varambally, S.; Cao, X.; Tchinda, J.; Kuefer, R., et al. Science. Vol. 310. New York, NY: 2005. Recurrent fusion of TMPRSS2 and ETS transcription factor genes in prostate cancer; p. 644-648.

Wang J, Cai Y, Ren C, Ittmann M. Expression of variant TMPRSS2/ERG fusion messenger RNAs is associated with aggressive prostate cancer. Cancer research 2006;66:8347–8351. [PubMed: 16951141]

Wang Q, Li W, Liu XS, Carroll JS, Janne OA, Keeton EK, Chinnaiyan AM, Pienta KJ, Brown M. A hierarchical network of transcription factors governs androgen receptor-dependent prostate cancer growth. Molecular cell 2007;27:380–392. [PubMed: 17679089]

Wang Q, Moncman CL, Winkelmann DA. Mutations in the motor domain modulate myosin activity and myofibril organization. Journal of cell science 2003;116:4227–4238. [PubMed: 12953063]

Yi YW, Kim D, Jung N, Hong SS, Lee HS, Bae I. Gadd45 family proteins are coactivators of nuclear hormone receptors. Biochemical and biophysical research communications 2000;272:193–198. [PubMed: 10872826]

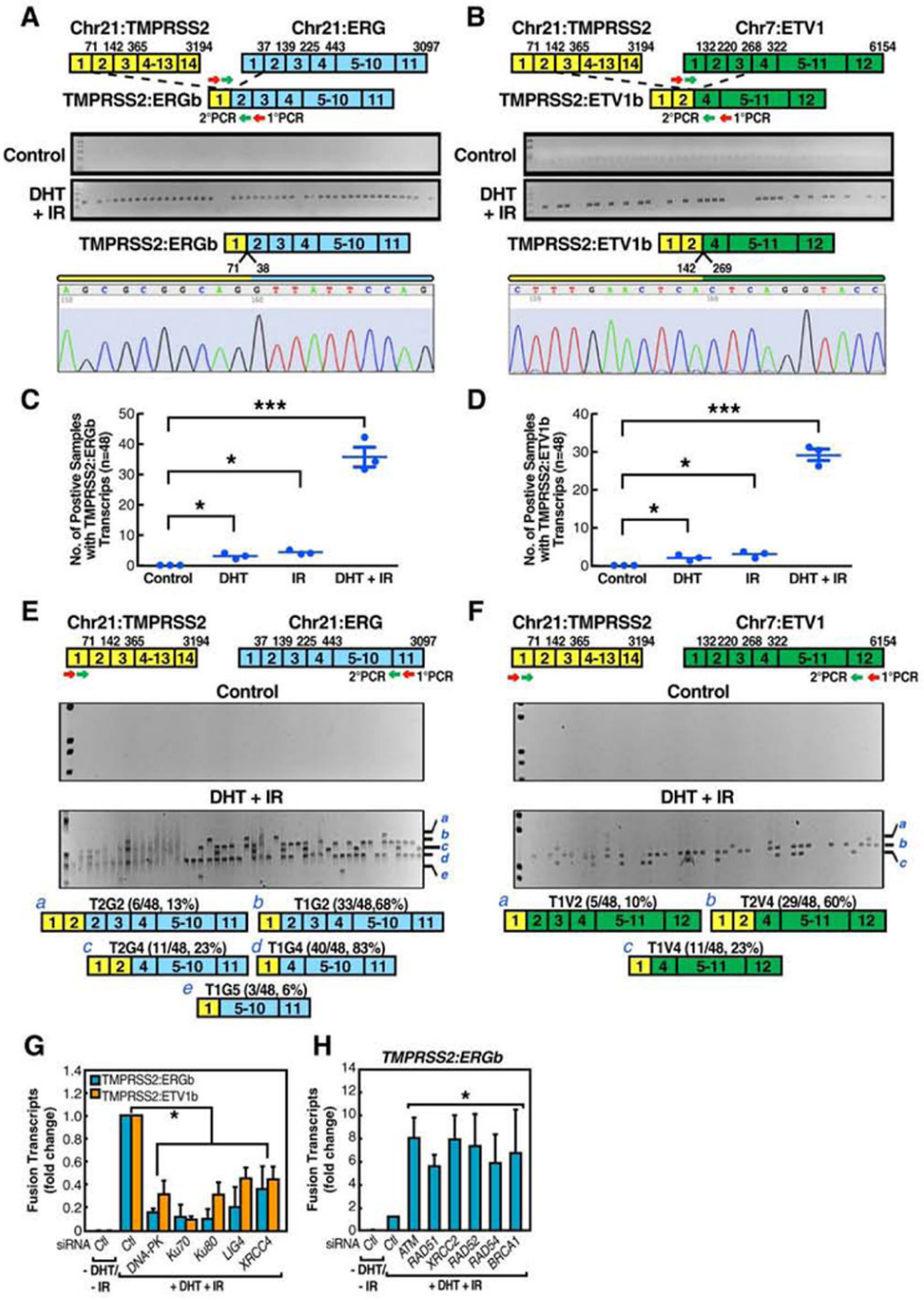

Figure 1. Liganded-AR and Genotoxic Stress Synergistically Induce Chromosomal Translocations in Prostate Cancer Cells

(**A** and **B**) Identification and characterization of induced *TMPRSS2:ERGb* and *TMPRSS2:ETV1b* translocations in LNCaP cells. Top: schematic structures for the *TMPRSS2*, *ERG*, and *ETV1* mRNA indicating exon positions. Middle: RT-PCR amplification of *TMPRSS2:ERGb* (A) or *TMPRSS2:ETV1b* (B) fusion transcripts from 48 individual cell samples. Bottom: confirmation of position and fusion sites by automated DNA sequencing. (**C** and **D**) Statistical analysis of DHT and IR induced *TMPRSS2:ERG* (C) and *TMPRSS2:ETV1* (D) translocations (n=3, ±SEM). (**E** and **F**) Identification and characterization of induced *TMPRSS2:ERG* (E) and *TMPRSS2:ETV1* (F) translocation isoforms in LNCaP

cells. Bottom: summary of distinct fusion types. (**G** and **H**) Involvement of DNA repair machinery in induced *TMPRSS2:ERGb* and *TMPRSS2:ETV1b* translocations by QPCR with indicated siRNAs (*n*=3, ±SEM).

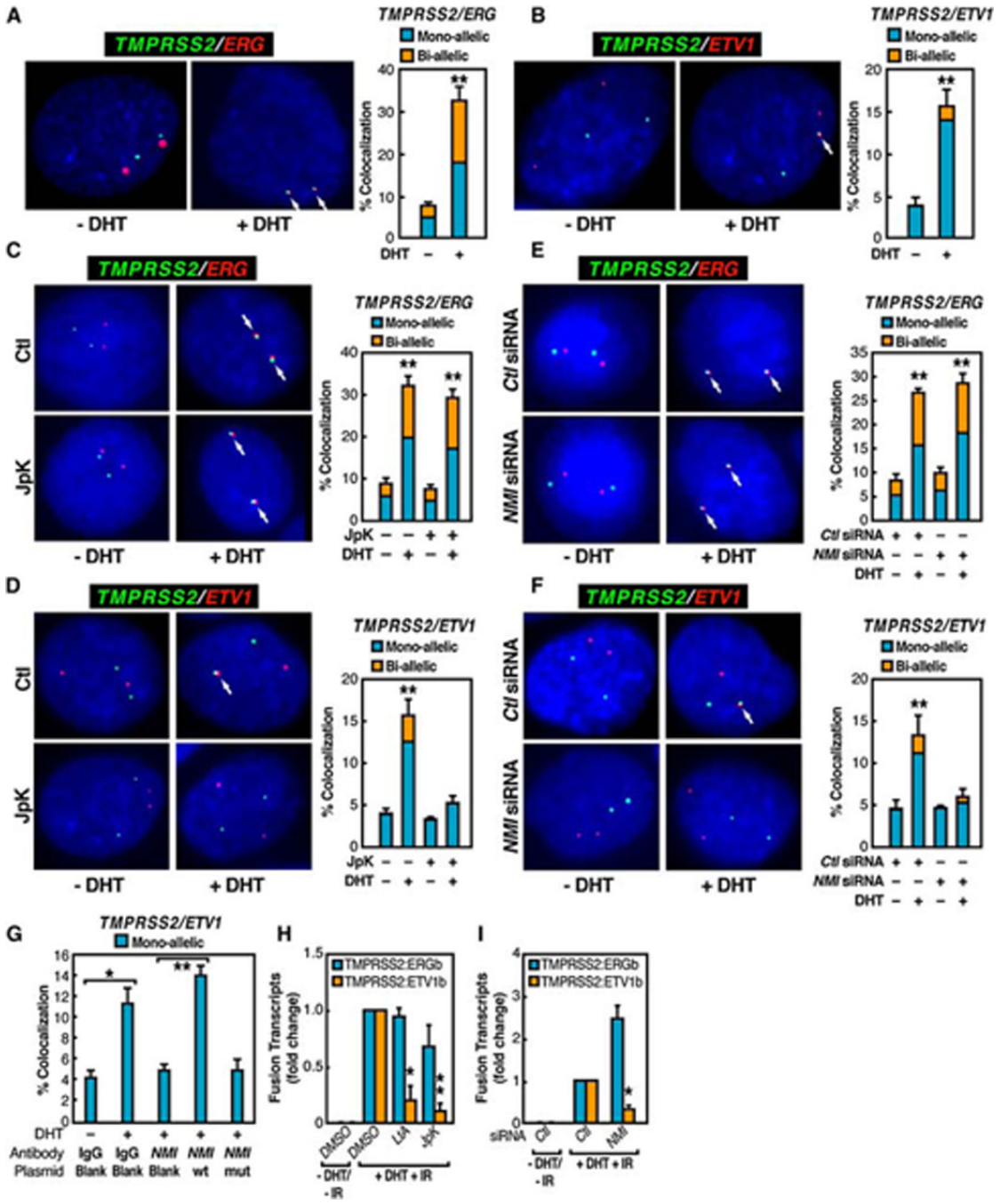

Figure 2. AR-Induced and Motor-Dependent Chromosomal Interactions of *TMPRSS2* and *ERG or ETV1* Loci

(**A** and **B**) Interphase FISH analysis on PrEC cells with *TMPRSS2* (green), *ERG* (red) (A), or *ETV1* (red) (B) probes. (**C** and **D**) Actin polymerization-dependent interchromosomal interactions. (**E** and **F**) Nuclear myosin-dependent interchromosomal interactions. (**G**) ATPase activity of NMI is required for DHT induced interchromosomal interactions. (**H** and **I**) Requirement of nuclear myosin/actin motor system for induced *TMPRSS2:ERGb* and *TMPRSS2:ETV1b* translocations in LNCaP cells pretreated with Latrunculin (LtA) or Jasplakinolide (Jpk) (H) or transfected with *NMI* siRNA (I) (*n*=3, ±SEM).

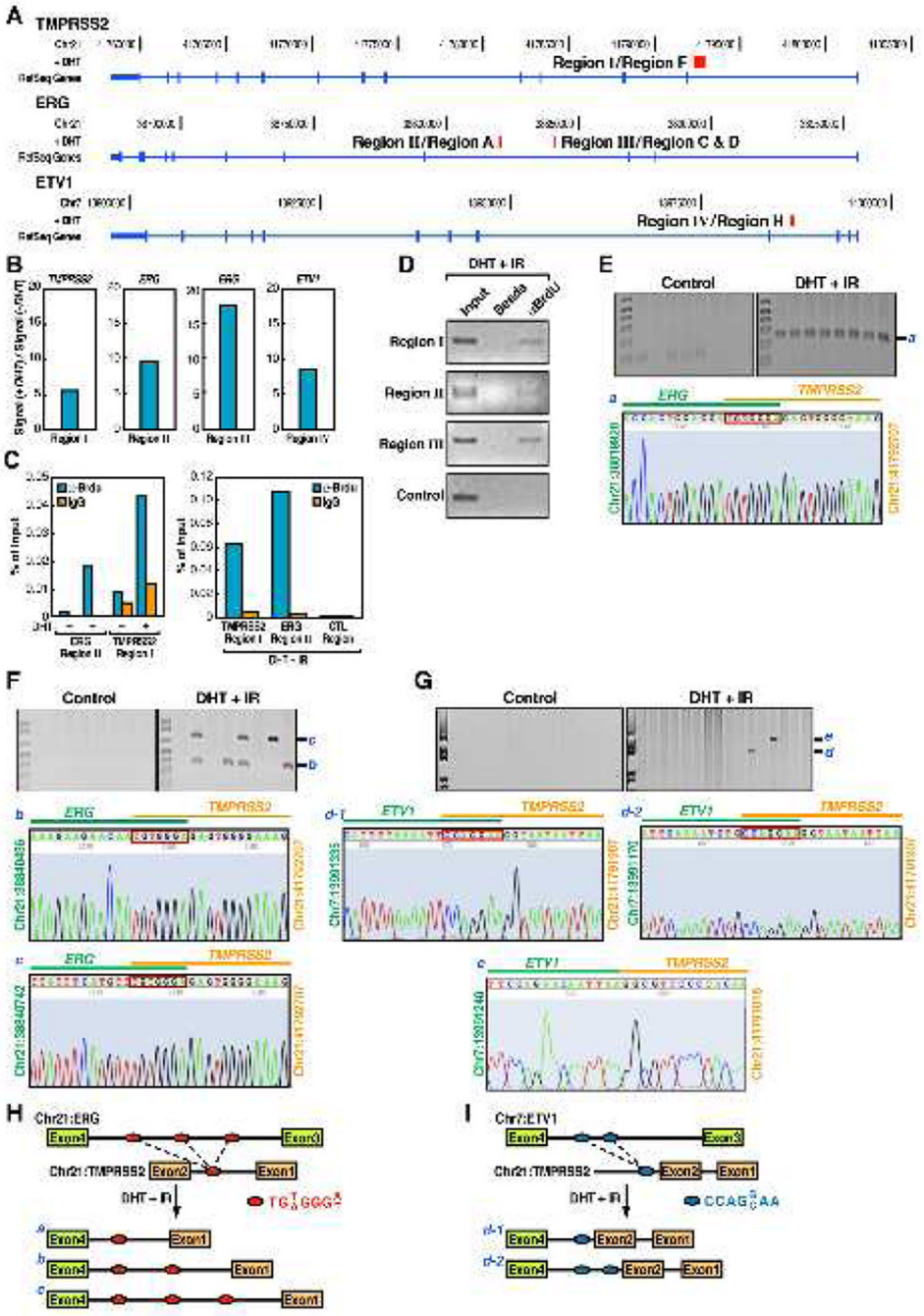

Figure 3. Identification of Breakpoints for *TMPRSS2:ERG* and *TMPRSS2:ETV1* Translocations

(**A**) The tracks display the human genome coordinates (hg18 assembly), red band: predicted potential DSBs based on ChIP-seq using anti-BrdU antibodies (see **Experimental Procedures**). Boxes: exons; lines: introns; Region I to IV: DNA break points within corresponding loci. (**B**) The fold change of the tag density in the double-strand break regions I, II, III and IV after DHT treatment. (**C** and **D**) Conventional ChIP analysis with anti-BrdU antibodies on *ERG* and *TMPRSS2* intronic break regions identified by ChIP-seq. **(E-G)** Identification and characterization of induced *TMPRSS2:ERG* and *TMPRSS2:ETV1* translocation breakpoints. Top: genomic DNA extracted from LNCaP cells either non-transfected (E) or co-transfected with *MeCP2* siRNA and FLAG-DOT1L expression vector (F

and G) was subjected to PCR amplification using primers flanking Region II and I (E), Region III and I (F), or Region IV and I (G). Bottom: automated DNA sequencing aligned to *ERG* or *ETV1* (green) and *TMPRSS2* (orange) with genomic position of starting and ending nucleotides shown. Red box: common sequence shared by *TMPRSS2* and *ERG* or *ETV1*. (**H** and **I**) Graphic illustration of translocation patterns corresponding to induced *TMPRSS2:ERG* (H) and *TMPRSS2:ETV1* (I) translocations. Potential break/fusion sites are shown as *Red oval*: *TMPRSS2:ERG*; *blue oval*: *TMPRSS2:ETV1*; dot line: distinct fusion patterns.

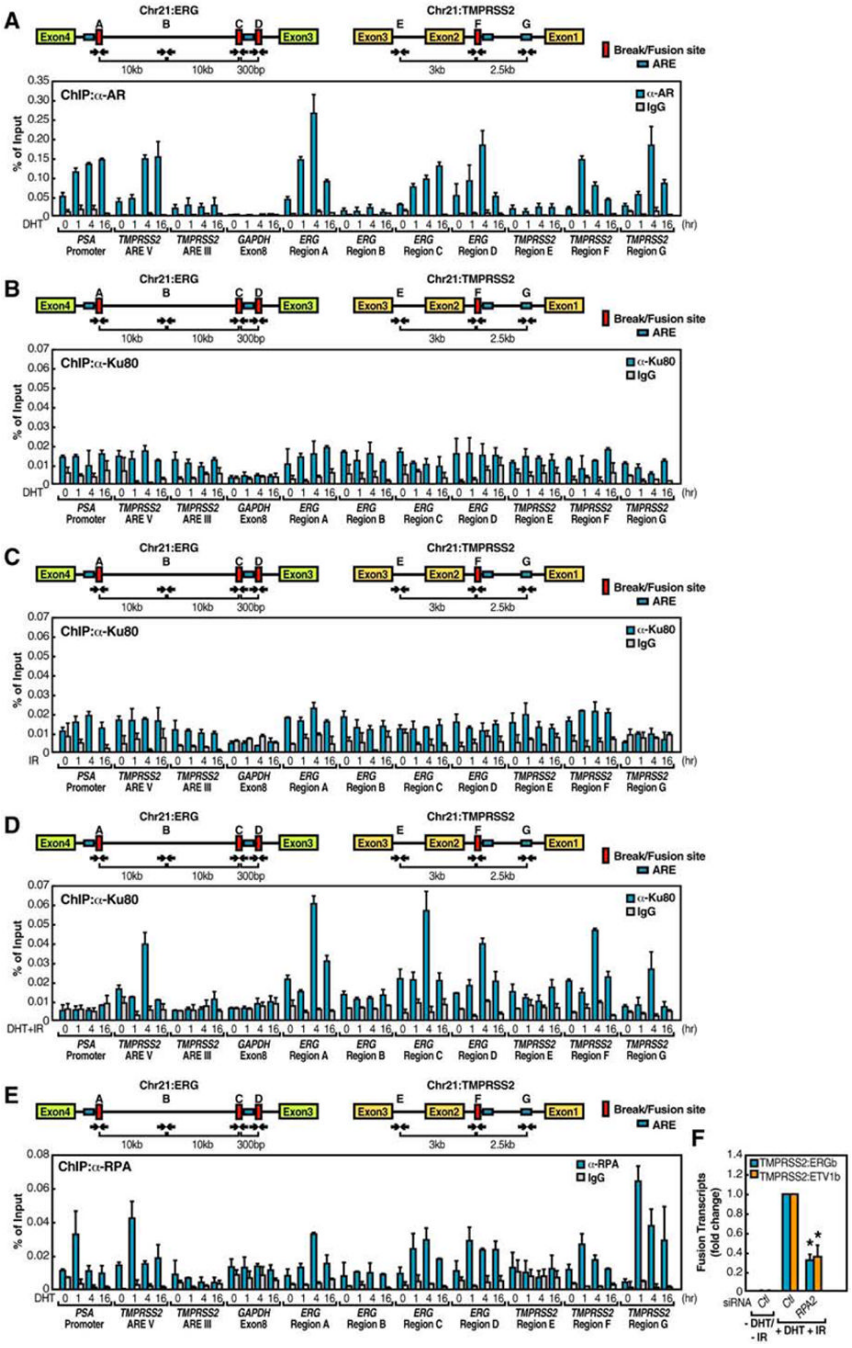

Figure 4. AR-Dependent Local Chromatin Structural Alteration Sensitizes to Site-Specific Genotoxic Stress-Induced DSBs

(**A**-**E**) Top: schematic diagram showing the relative positions of break/fusion sites and potential AREs located on *ERG* and *TMPRSS2* loci. *Blue boxes*, potential AREs; *red boxes*, break/fusion sites; *black arrows*, relative positions of PCR primers. Bottom: LNCaP cells were treated with DHT (10^{-7} M) (A), DHT (10^{-7} M) (B), IR (50 Gy) (C) or both (D) and DHT (10^{-7} M) (E) for time courses as indicated. ChIP analyses were performed with indicated antibodies on indicated regions (n=2, ±SEM). (**F**) Examination of *TMPRSS2:ERGb* and *TMPRSS2:ETV1b* fusion transcripts with *RPA2* siRNAs (n=3, ±SEM).

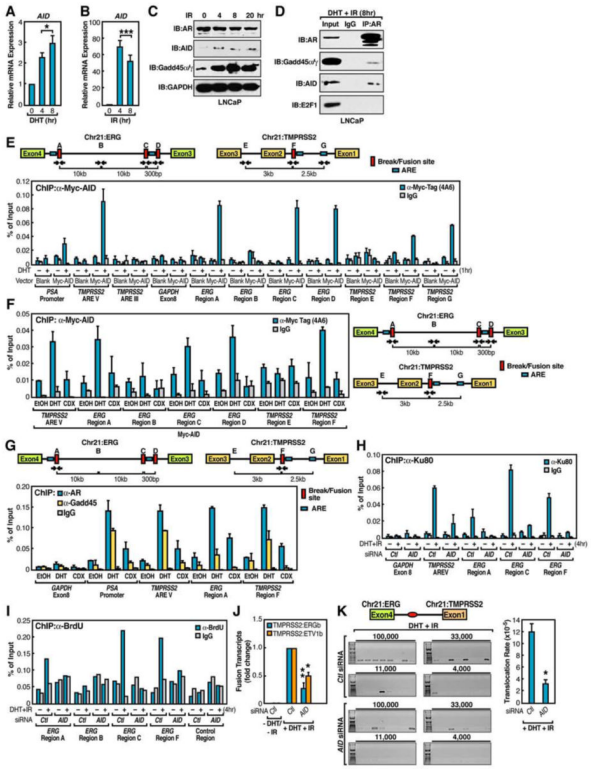

Figure 5. Mechanisms that Initiate Extended DNA Breaks in AR-Dependent Tumor Translocations

(**A-C)** Induction of *AID* expression by AR agonist and genotoxic stress. (*n*=3, ±SEM). (**D**) DHT-dependent interaction between AR and AID. Immunoprecipitates of anti-AR were subjected to immunoblotting analysis with indicated antibodies. Immunoblotting of E2F1 was included as negative control. (**E**) Ligand-dependent Myc-AID recruitment to AR-binding sites (*n*=2, ±SEM). (**F** and **G**) The recruitment of AID and Gadd45 to AR binding sites is mediated by liganded receptor. LNCaP cells were treated with ethanol (EtOH), DHT (10^{-7} M), or Bicalutamide (CDX, 10 μM) for 1hr followed by ChIP analyses with anti-Myc (F) or anti-AR and anti-Gadd45 (G) antibodies on indicated regions (*n*=2, ±SEM). (**H** and **I**) AID contributes to DSBs generation. ChIP analyses were performed on control siRNA or *AID* siRNA transfected, DHT+IR treated (4hr) LNCaP cells with anti-Ku80 antibodies (*n*=2, ±SEM) (H) or anti-BrdU antibody following BrdU labeling by TdT (I) on indicated regions. (**J**) Examination of *TMPRSS2:ERGb* and *TMPRSS2:ETV1b* fusion transcripts in LNCaP cells transfected with *AID* siRNA (*n*=3, ±SEM). (**K**) Left: representative agarose gels with PCR products corresponding to *TMPRESS2:ERGa* translocations (as illustrated in Figure 3H band *a*). The genomic DNA of control or *AID* siRNA transfected LNCaP cells were subjected to PCR using primers flanking ligation site (*red oval*). Right: Statistical analysis (*n*=3, ±SEM).

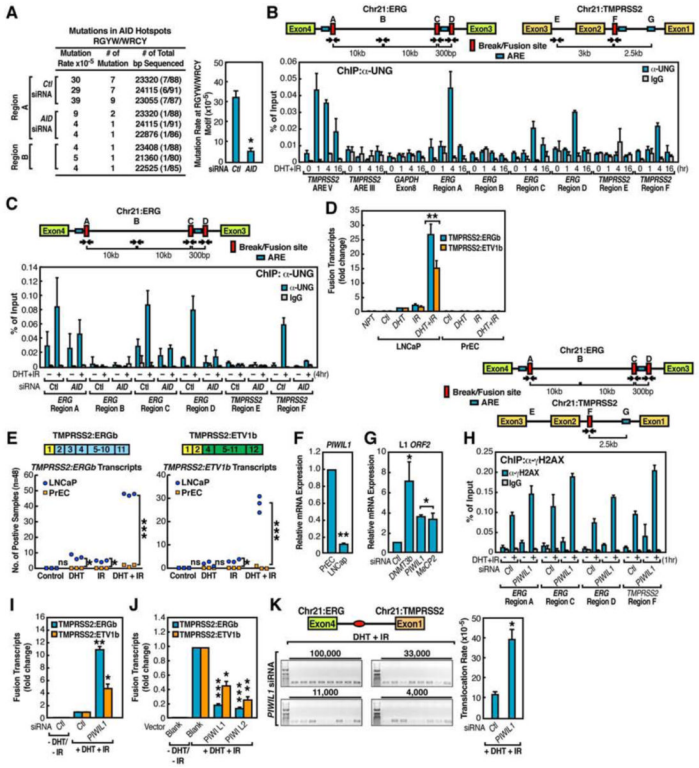

Figure 6. Protective Effects of PIWIs on Chromosomal Translocation

(**A**) Left: summary of identified RGYW/WRCY motif related mutation. The fusion chromatins of ERG region A in control siRNA and *AID* siRNA samples or ERG region B were amplified as in Figure 3E. Right: statistics analysis (*n*=3, ±SEM). (**B**) Ligand-dependent UNG recruitment to intronic regions of *TMPRSS2* and *ERG* loci. (**C**) Recruitment of UNG to translocation regions is AID dependent. **D**) Quantitation of induced *TMPRSS2:ERGb* and *TMPRSS2:ETV1b* fusion transcripts in LNCaP or PrEC cells. NPT: normal prostate tissue. (**E**) Statistical comparison of induced *TMPRSS2:ERGb* (left) and *TMPRSS2:ETV1b* (right) fusion transcripts LNCaP and PrEC cells (48 samples *per* group and *n*=3, ±SEM). (**F**) The relative expression level of *PIWIL1* in LNCaP and PrEC cells. (**G**) The expression level of LINE-1 *ORF2* was examined in PrEC cells transfected with indicated siRNAs. (**H**) *PIWIL1* knockdown enhances γH2AX enrichment at intronic *ERG* and *TMPRSS2* break/fusion sites. (**I** and **J**) Examination of *TMPRSS2:ERGb* and *TMPRSS2:ETV1b* fusion transcripts in LNCaP cells electroporated with *PIWIL1* siRNA (I) or indicated plasmids (J) (*n*=3, ±SEM). (**K**) Left: representative agarose gels with PCR products corresponding to *TMPRESS2:ERGa* translocations (as illustrated in Figure 3H band *a*). Right: Statistical analysis (*n*=3, ±SEM).

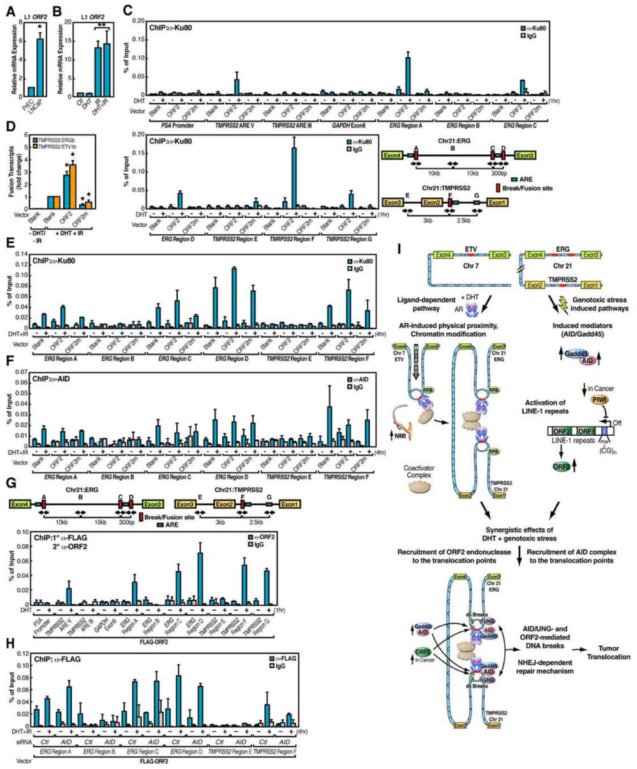

Figure 7. PIWI Regulated LINE-1 ORF2 Endonuclease Contributes to Chromosomal Translocations

(**A**) The relative expression level of LINE-1 *ORF2* in LNCaP and PrEC cells. (**B**) IR-dependent induction of LINE-1 *ORF2* expression (*n*=3, ±SEM). (**C**) Overexpression of LINE-1 *ORF2* enhances Ku80 enrichment at intronic *ERG* and *TMPRSS2* break/fusion sites. (**D**) Examination of *TMPRSS2:ERGb* and *TMPRSS2:ETV1b* fusion transcripts in LNCaP cells electroporated with indicated plasmids (*n*=3, ±SEM). (**E** and **F**) ORF2 contributes to DSBs generation independent of AID. ChIP analyses with anti-Ku80 (E) or anti-AID (F) antibodies were performed in LNCaP cells electroporated with indicated plasmids (*n*=2, ±SEM). (**G**) Recruitment of LINE-1 ORF2 to translocation regions. ChIP analyses with anti-FLAG followed by anti-ORF2 antibodies were performed in LNCaP cells electroporated with FLAG-ORF2 plasmid (*n*=2, ±SEM). (**H**) The recruitment of ORF2 is independent of AID. ChIP analyses with anti-FLAG antibodies were performed in LNCaP cells electroporated with *AID* siRNA and FLAG-ORF2 plasmid (*n*=2, ±SEM). (**I**) Schematic illustration of molecular mechanisms of nuclear receptor-dependent non-random chromosomal translocations.